*Journal of Ceramic Processing Research. Vol. 20, Special. 1, pp. s100~s108 (2019)*
*(Received 26 December 2018, Received in revised form 25 June 2019, Accepted 5 July 2019)*

J O U R N A L O F
Ceramic
Processing Research

# Feasibility study of inorganic anti-corrosion agents with self-healing capabilities for reinforced concrete structures

**Hee Seok Lee and Kwang Ho Sho***
*Department of Architectural Engineering, Wonkwang University, Iksan 54538, Korea*

**This study focuses on development of anti-corrosion agent with crack self-healing capabilities for reinforced concrete structures. New inorganic mix-proportions with swelling and expansion properties for crack self-healing capabilities were designed to conduct such as paste, mortar and concrete experiments. For the flow tests, W/C ratio of 0.35 was used for the cementitious paste. In case of mortar test, W/C ratio of 0.5 and C/S ratio of 1:3 were used. In case of concrete, mixing proportions of concrete; a W/B ratio of 52% and S/A ratio of 48% were applied to all concretes for the fluidity test, compressive strength, corrosion-ratio of steel bar on the NaCl 6% addition to mix-proportion. EPMA results revealed particular trends in the chemical composition, such as the formation of calcium alumina silicate materials in cracks. Moreover, Cl ions was decreased from surface to internal area in the concrete by self-healing effects. From these results, it was confirmed the fluidity, compressive strength, and anti-corrosion effect with self-healing capabilities.**

**Key words: Anti-corrosion agent, Crack, Self-healing, Swelling, Expansion.**

## Introduction

Concrete is widely used in building structures and performs strongly against compressive force, but weakly against tension. Reinforced concrete and pre-stressed concrete, which reinforces the weak tensile strength, are commonly used. Concrete containing rebar is strongly alkaline, which protects the rebar, but over long periods of time, structural performance is reduced due to the penetration of chlorides, carbon dioxide, sulfates, and moisture. When reinforced concrete is used in bridges built in coastal areas, the passive film is easily destroyed by salt damage, resulting in rebar corrosion. If rebar corrosion progresses, cracks can occur in the concrete and thermal factors flowing through the cracks further accelerate rebar. This greatly reduces the durability of the concrete structure and countermeasures against this phenomenon are needed [1-2].

Typically, an epoxy coating and cement paste are used for rebar corrosion control in reinforced concrete structures. However, even though epoxy coating exhibits excellent corrosion control properties and adhesion to the rebar, problems with adhesion between the epoxy coating layer and concrete matrix persist. As such, concerns regarding the removal of the epoxy from the interface and increased corrosion are well-founded. In addition, when uncoated rebar or rebar with coating chips peeling off is exposed to the outside, the corrosion rate of the rebar can increase rapidly due to differences in electrical conductivity [3-5].

Cement paste anti-corrosion materials normally form a passive film on the rear surface through the inherently strong alkalinity of the cement. However, a problem often occurs when various thermal factors in harsh environments (chlorine ions, carbon dioxide gas, etc.) flow in through cracks and easily destroy the passive film.

Recently, self-healing technology for reducing micro-cracks in concrete has attracted significant interest in South Korea. Self-healing technology is being developed as a novel concrete material because it can promote durability and increase the concrete lifespan and reduce maintenance costs. If this self-healing technology can be applied to cement paste anti-corrosion material, it could block the invasion of thermal factors that can infiltrate through micro-cracks and resolve maintain the passive film. In addition, the properties of the self-healing materials can make the internal structure of the concrete compact and watertight, which can improve the durability [6-10].

Therefore, this study aimed to develop an inorganic anti-corrosion material for reinforced concrete structures with salt damage resistance and micro-crack self-healing properties and to evaluate its basic performance in terms of corrosion control and chloride binding [11-15].

## Experimental Procedure

### Materials

Six types of mix-proportions were used with Ordinary

*Corresponding author:
Tel : +82-63-850-6707
Fax: +82-63-843-0782
E-mail: wk2000@nate.com

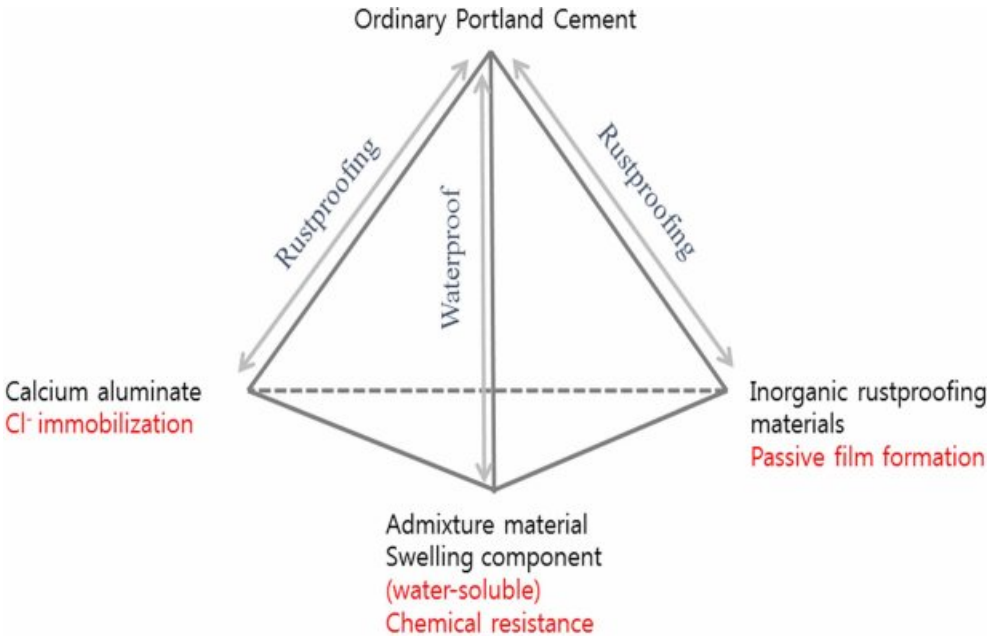


**Fig. 1.** Design of inorganic anti-corrosion materials with self-healing capability.

Portland Cement (OPC) in binary and ternary mix in this study. Table 1 shows the mix-proportions of paste tests in this research. Blast furnace slag (GBS), swelling materials (BN), expansion materials (CSA) were used for the self-healing capabilities based on previous researches as shown in Fig. 1 [16-20]. $LiNO_2$, $Ca(NO_2)_2$ and anti-rust agent (made in Japan) were used for the anti-corrosion test. Acrylate copolymers were also used for this investigation. The chemical compositions of are given in Table 2. In case of mortar and concrete test, Table 3 and Table 4 show mix-proportion in each case. Slump flow of concrete was measured at the initial point by KS F 2402, air contents was investigated by KS F 2421. The compressive

**Table 3.** Mixing proportion of mortar

| Kind | W/C (%) | Unit weight (kg/m$^3$) | | | | |
|---|---|---|---|---|---|---|
| | | W | S | OPC | Rust inhibitor | NaCl |
| P | 50 | 246.30 | 1492.73 | 463.05 | - | 29.55 |
| MO | | | | 416.75 | 46.30 | 29.55 |
| M1 | | | | 416.75 | 46.30 | 29.55 |
| M2 | | | | 416.75 | 46.30 | 29.55 |
| M3 | | | | 416.75 | 46.30 | 29.55 |
| M4 | | | | 416.75 | 46.30 | 29.55 |
| M5 | | | | 416.75 | 46.30 | 29.55 |

**Table 1.** Chemical composition of mix-proportion

| Kind | W/C (%) | Unit weight (kg/ m$^3$) | | | | | | | |
|---|---|---|---|---|---|---|---|---|---|
| | | C | GBS | BN | CSA | $LiNO_2$ | $Ca(NO_2)_2$ | Anti -rust agent | P |
| P | 35% | 1000 | 0 | 0 | 0 | 0 | 0 | 0 | 0 |
| M0 | | 0 | 0 | 0 | 0 | 0 | 0 | 1000 | 0 |
| M1 | | 740 | 100 | 40 | 20 | 50 | 0 | 0 | 50 |
| M2 | | 740 | 100 | 40 | 20 | 0 | 50 | 0 | 50 |
| M3 | | 690 | 100 | 40 | 20 | 50 | 50 | 0 | 50 |
| M4 | | 650 | 100 | 60 | 40 | 50 | 50 | 0 | 50 |
| M5 | | 600 | 100 | 60 | 40 | 50 | 100 | 0 | 50 |

**Table 2.** Chemical composition of acrylate copolymers

| Chemical composition (%) | | | | | | |
|---|---|---|---|---|---|---|
| Component | Appearance | Tg (°C) | Average particle size | Volatile matters | pH | Density (g/cm$^3$) |
| Pure acrylate copolymer | white uniform powder | 0 | approx. 100? | 2% or below | 7±1 | 0.5±0.1 |

**Table 4.** Mixing proportion of concrete

| Kind | Design strength (MPa) | W/B (%) | S/a (%) | W (kg) | Unit weight (kg/m$^3$) | | | | | |
|---|---|---|---|---|---|---|---|---|---|---|
| | | | | | Binder (kg) | | NaCl | Fine aggregate (kg) | Coarse aggregate (kg) | Water Reducer (kg) |
| | | | | | OPC | Rust inhibitor | | | | |
| P | 24 | 52 | 48 | 180 | 325.24 | - | 20.76 | 826 | 902 | 1.73 |
| M0 | | | | | 292.72 | 32.52 | 20.76 | | | |
| M1 | | | | | 292.72 | 32.52 | 20.76 | | | |
| M2 | | | | | 292.72 | 32.52 | 20.76 | | | |
| M3 | | | | | 292.72 | 32.52 | 20.76 | | | |
| M4 | | | | | 292.72 | 32.52 | 20.76 | | | |
| M5 | | | | | 292.72 | 32.52 | 20.76 | | | |

strength of mortar and concrete were also measured by KS F 5105 and KS F 2405 after 3, 7 and 28 days.

## Estimation method of anti-corrosion effects

Anti-corrosion agents for reinforced concrete structures were also measured by KS F 2561. The corrosion-ratio of steel bars in the concrete was measured by the Vernier calipers after splitting of specimens on the curing 28 days as shown in Fig. 2.

**Fig. 2.** Measurement of corrosion-ratio after splitting of specimens.

## Estimation method of crack self-healing behavior

Cementitious composite paste with anti-corrosion ability cylinders 5f X 10 cm in size were prepared with W/C 40%. They were cured for 7 days and then artificially cracked in order to clarify the self-healing behavior as shown in Fig. 3. Crack width was controlled for 0.1mm. After cracking, the specimens were again water cured for 7 days. The water pass test was investigated during 28 days by JIS A 6909: 2014. Cracks were measured after water pass test as shown in Fig. 4. The water flow through the crack was measured after filling water in the polyvinyl chloride pipes. The elapsed time was recorded for 5 mins, when the surface of the water decreased. This measurement was conducted on the 0, 1, 3, 7, 14, 21, 24 and 28 days. To observe the damaged interface between cracks, the pre-damaged specimens were cut using oil as a lubricant and polished. A digital microscopy and electron probe micro-analyzer (Shimadzu EPMA-8705) were used to investigate the morphology of the cross section.

**Fig. 3.** Assessing self-healing through cracks in cementitious paste.

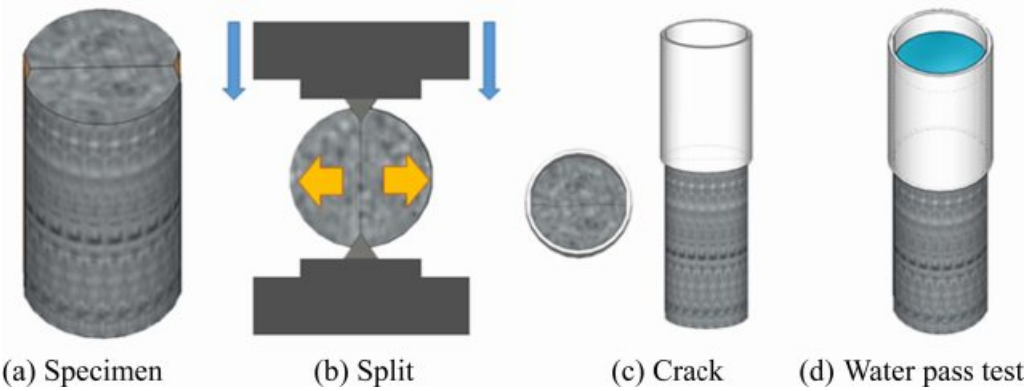


**Fig. 4.** Experimental procedure for the water pass test.

## Results and Discussion

### Physical properties of inorganic anti-corrosion pastes

Fig. 5 shows behaviors such as initial setting time, final setting time and flow of various inorganic an-corrosion pastes. In case of M0 and M1, their setting time are similar to that of Plain as shown in Fig. 5(a) and Fig. (b). However, in case of M2, M3, M4, and M5, they are decreased over 40% on both initial and final setting time due to the coagulation phenomena of $LiNO_2$ and $Ca(NO_2)_2$ occurring rapidly. Therefore, mix-proportions with $LiNO_2$ and $Ca(NO_2)_2$ should be reconsidered in order to compensate for setting and flow loss. Fig. 5(c) shows the fluidity results of cementitious composite pastes with anti-corrosion agents. The addition of blast furnace fine powders and swelling materials resulted in rapid flow loss, because of its water adsorption in system. Furthermore, in case

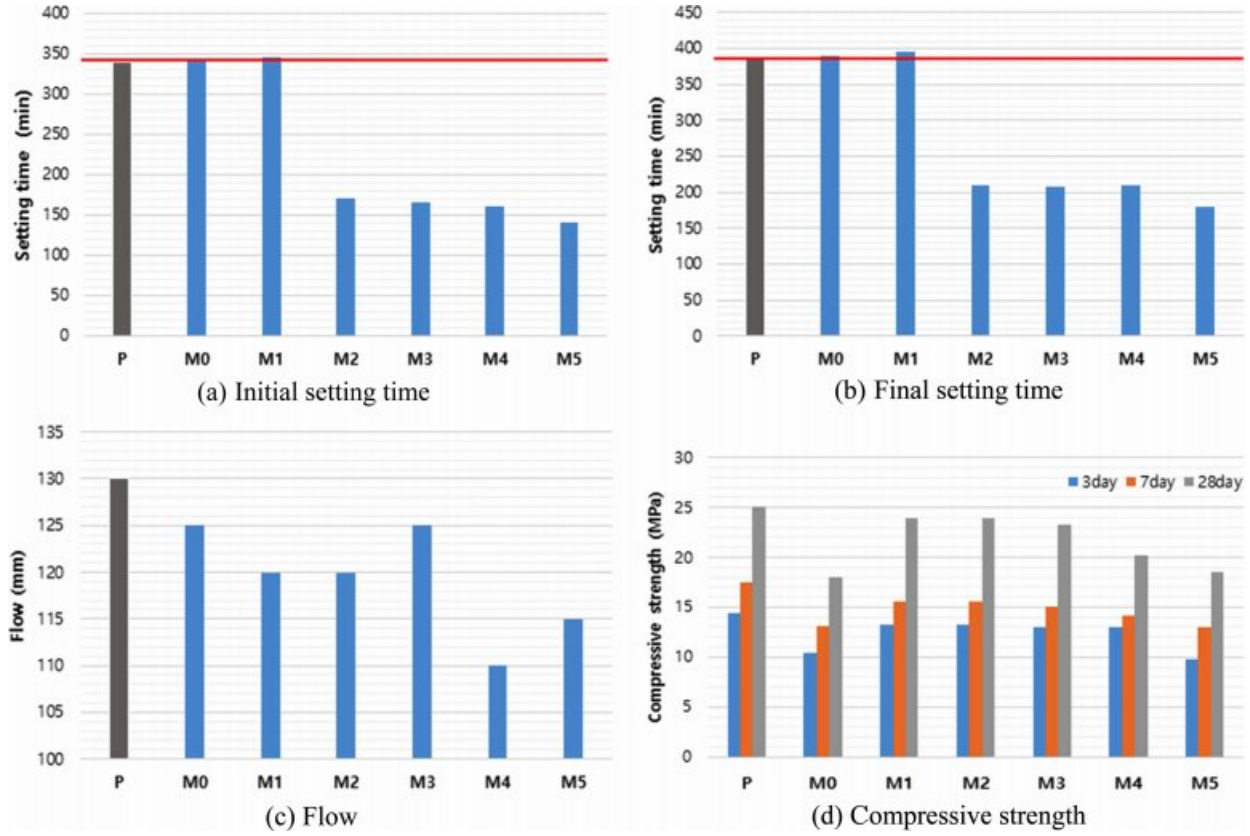


**Fig. 5.** Physical properties of inorganic anti-corrosion pastes.

of compressive strength, it can be seen that anti-corrosion pastes exhibits lower compressive strength to Plain as shown in Fig. 5(d). This means that the addition of a lot of anti-corrosion agents also decreased the compressive strength due to replacement of cement amounts in the systems. In case of M1, M2, M3, M4 and M5, they shows high compressive strength compared to M0, because of blast furnace find powders and expansion agents in terms of long-age compressive strengths. From these results, it can be said that anti-corrosion agents were not effective in solving the incompatibility problem. However, some mix-proportions such as M1, M2 and M3 shows similar to that of Plain in terms of setting time and compressive strength. Therefore, these are premixed again with retarding agent for anti-corrosion and self-healing behavior of mortar and concrete.

**Verification of anti-corrosion effects on mortar and concrete**

Fig. 6 shows the effect of the addition of the retarding agent [$(CH_2COONA)_2 \cdot 2H_2O$] on the fluidity for mortar and concrete. Initial target flow was 200mm for mortar. In case of the addition of retarding agent, it shows similar retention effects of Plain (P) compared to previous past tests. In case of concrete, table 4 shows the mixing proportions of concrete; a W/B ratio of 52% and S/A ratio of 48% were applied to all concretes. Slump flow of concrete was measured at the initial point. In this case, it shows similar mortar results. The average air contents were around 6%. Fig. 7(a) shows the development of the compressive strength of the mortars that contained anti-corrosion agents. The mortars that contained M1, M2 and M3 exhibited similar compressive strength of Plain. However, the compressive strengths of M0, M4 and M5 exhibited lower compressive strength than that of Plain because of the decrease of cement amounts by the replacement. Fig. 7 (b) shows the compressive strength of the concrete. In case of concrete, they shows the similar results of mortar cases. Especially, M1, M2 and M3 exhibited 24 Mpa of target compressive strength, these are similar results of mortar. Fig. 8 shows the corrosion rate of steel bar in the mortar with various inorganic anti-corrosion agents. In case of anti-rust agents coating method, various inorganic anti-corrosion agents were coated on the steel bars with f10 X 200mm size. After they were cured during 24hours, they were used to normal concrete mixing with NaCl 6% solution. In case of anti-rust substitution method, cements were replaced by 10% of inorganic anti-corrosion agents both mortar and concrete. These results show that M3,

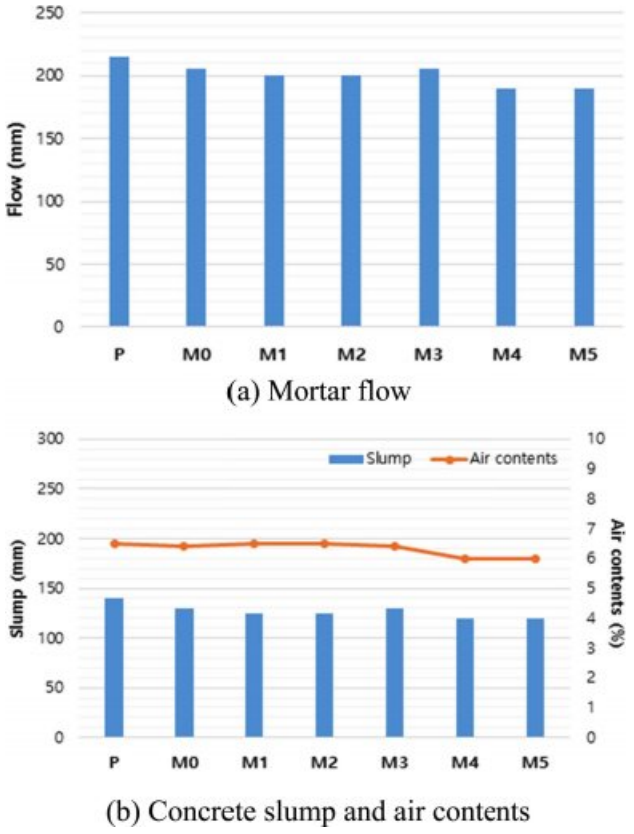


**Fig. 6.** Effects of retarding agent on the fluidity for mortar and concrete.

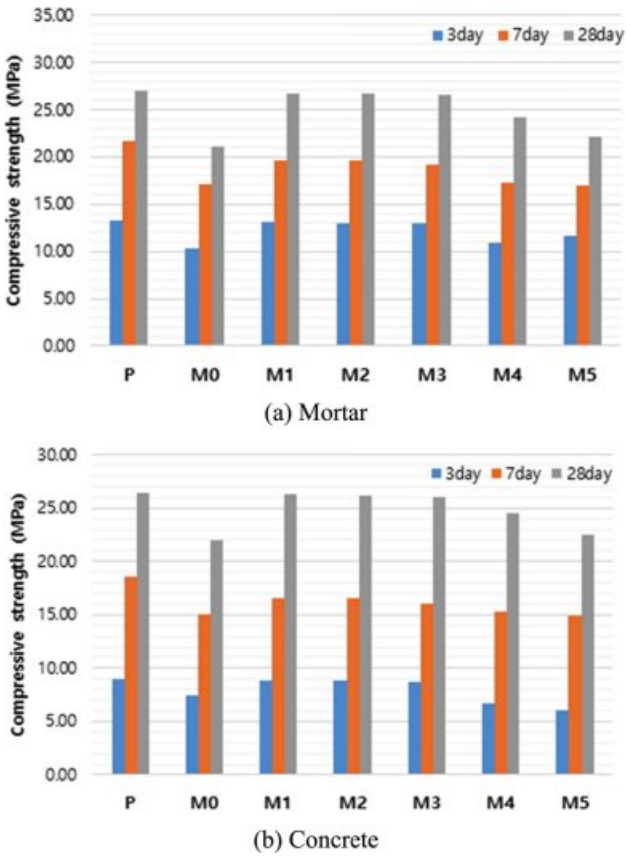


**Fig. 7.** Compressive strength behaviors of mortar and concrete.

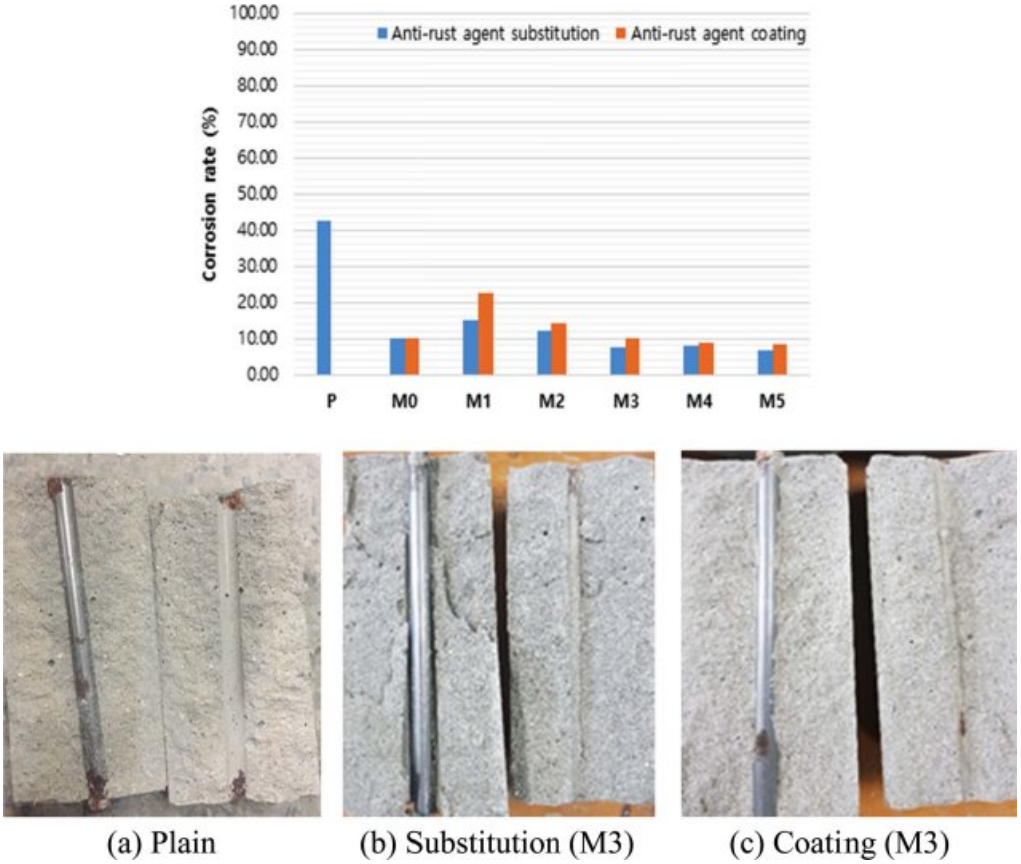


**Fig. 8.** Corrosion rate (%) of steel bars in the mortar matrix.

M4 and M5 appears to be an effective anti-corrosion behaviors compared to Plain as shown in Fig. 8(a) and Fig. 8(b), respectively. Especially, anti-rust substitution methods exhibited the best performance compared to anti-rust agent coating methods as shown in Fig. 8(c) and Fig. 8(d). It seems that the pore structures of mortar were denser than those of Plain by effective of swelling and expansion mechanism of self-healing materials. Therefore, it shows more good performances in terms of the protection of NaCl immersion. Fig. 9 shows the corrosion rate of steel bar in the concrete with various inorganic anti-corrosion agents. These results showed similar that of mortar. Especially, M3, M4 and M5 also appears to be an effective anti-corrosion behaviors compared to Plain as shown in Fig. 9(a) and Fig. 9(b) in case of concrete specimens. However, in case of corrosion rate on concrete specimens, there are clear differences between anti-rust agent substitution method and anti-rust agent coating method. Effects of anti-corrosion on the substitution method improved by over 20% compared to coating method. It especially seemed that pore size of concrete was bigger than that of mortar. Therefore, there were more easily to diffuse NaCl to matrix of concrete. Fig. 9(c) and Fig. 9(d) show the difference of corrosion status between substitution method and coating method in case of M3 on concrete specimens clearly.

From these results, it can be said that inorganic anti-corrosion agents with self-healing materials were effective in anti-corrosion. Especially, M3, M4 and M5 showed best performance. M3 series were selected for the verification of self-healing capabilities by considering previous results such as fluidity, compressive strength and anti-corrosion. It was studied in detail in the following section.

## Verification of self-healing capabilities of anti-corrosion agents

Fig. 10(a) and Fig. 10(b) show the healing process under water supply on the cracked Plain specimen and M3 specimen. In order to develop anti-corrosion materials with self-healing capabilities [9-10], cementitious composite pastes of M3 with W/C ratio of 0.4 were used. They were cured for 7 days and then artificially cracked in order to clarify the self-healing behavior. Crack width was controlled for 0.1mm. After cracking, Plain and M3 specimens were again water cured for 7 days. In case of Plain, after 7 days curing, the crack still remained even though the specimen was recurred under water immersion condition for 28 days. However, In case of M3 specimen with swelling and expansion materials, it was self-healed perfectly after re-curing

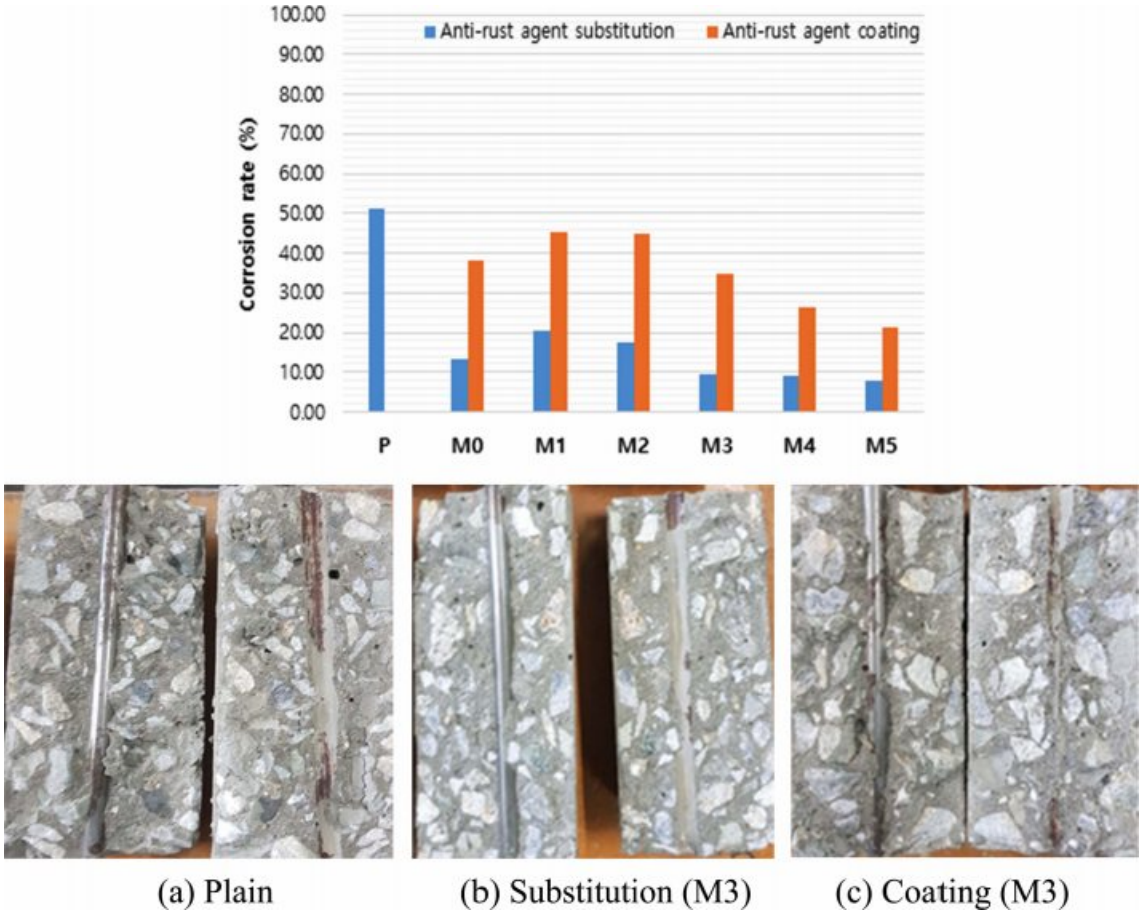


**Fig. 9.** Corrosion rate (%) of steel bars in the concrete matrix.

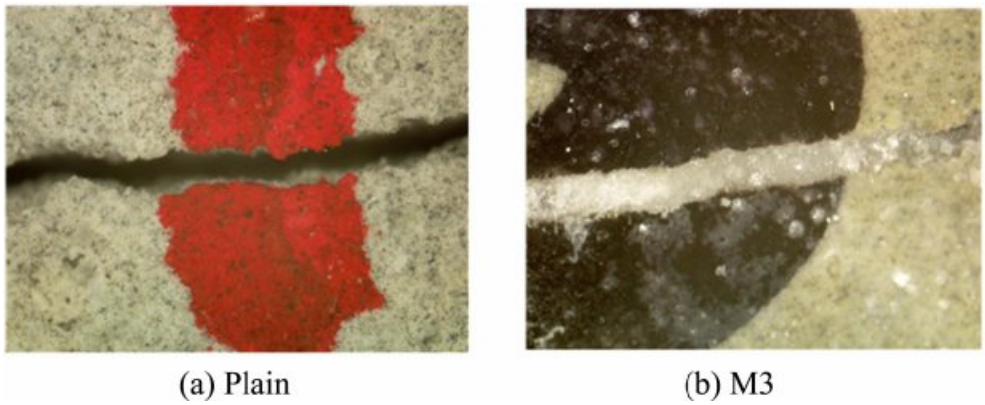


**Fig. 10.** Self-healing behavior of inorganic anti-corrosion agent with swelling and expansion materials (Crack width = 0.1 mm).

for 7 days. This recovery appeared to include self-healing behavior such as the swelling effect, expansion effect and re-crystallization as mentioned above [8-10].

Fig. 11 shows the results of water pass test in case of Plain and M3. Water pass test was investigated during 28 days. The elapsed time was recorded for 5 mins, when the surface of the water decreased. In case of Plain, the water leakage was decreased around 5.6% during 28 days, However, in case of M3, it was decreased around 20% during 3 days. Especially, M3 exhibited that it was decreased dramatically after 7 days. Finally, water leakage amounts of M3 was decreased around 60% during 28days compared to that of Plain. This indicates that M3 incorporating swelling and expansion materials has a high potential for self-healing capabilities with anti-corrosion effects.

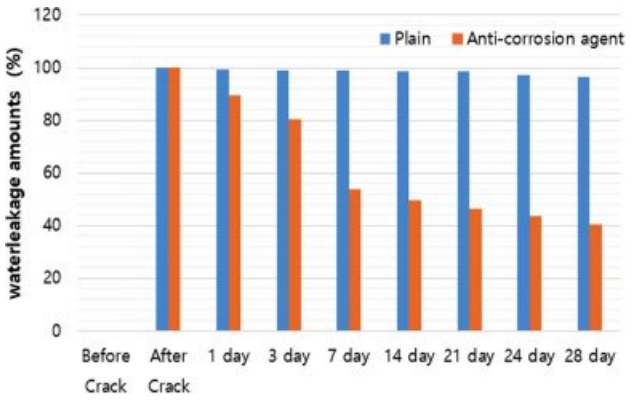


**Fig. 11.** Waterproof effects of inorganic anti-corrosion agent after water pass test.

Fig. 12 shows morphology, shape and size of rehydration products within cracks were investigated using electron probe microanalysis (EPMA). Fig. 12(a) shows crack area of M3 specimen. In particular, re-hydration products were mainly found to comprise calcium alumina silicate materials as shown in the X-ray mapping results from the polished section [Fig. 12(b), (c) and (d)]. Fig. 13 shows that Cl ions were spread from surface to internal area. However, Cl ions on the M3 specimen was decreased. Therefore, the relationship between self-healing capabilities and reasonable anti-corrosion agents should be considered in detail in order to understand the self-healing behavior of M3. Thus, a suitable swelling materials, mineral admixture and anti-corrosion agent should be carefully considered in the design of concrete to maximize their healing capacity. Therefore, verification of self-healing in an actual structure is essential and the cast materials will be studied continuously for the future works.

## Conclusions

In this study, the new method of anti-corrosion agent with self-healing capabilities design to repair cracks was suggested, and the anti-corrosion properties using swelling and expansion materials were investigated.

1) In case of physical properties of inorganic anti-corrosion paste, mix-proportions with $LiNO_2$ and $Ca(NO_2)_2$ should be reconsidered in order to compensate for setting time and flow loss.

2) In case of water pass test, some mixtures with self-healing agents exhibited that water leakage amounts was decreased around 60% during 28 days. Furthermore, EPMA results revealed particular trends in the in the chemical composition, such as the formation of calcium alumina silicate materials in cracks. Moreover, Cl ions was decreased from surface to internal area by self-healing effects.

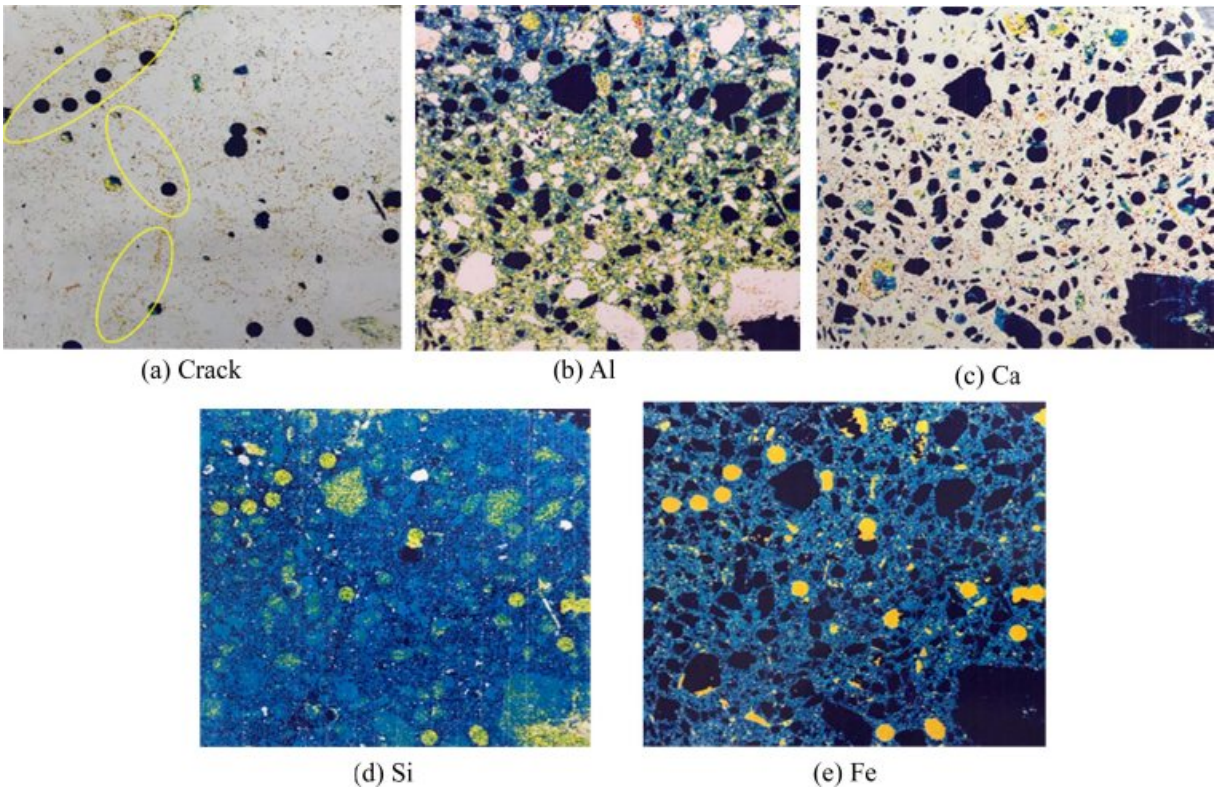


**Fig. 12.** Electron probe microanalysis (EPMA) after self-healing.

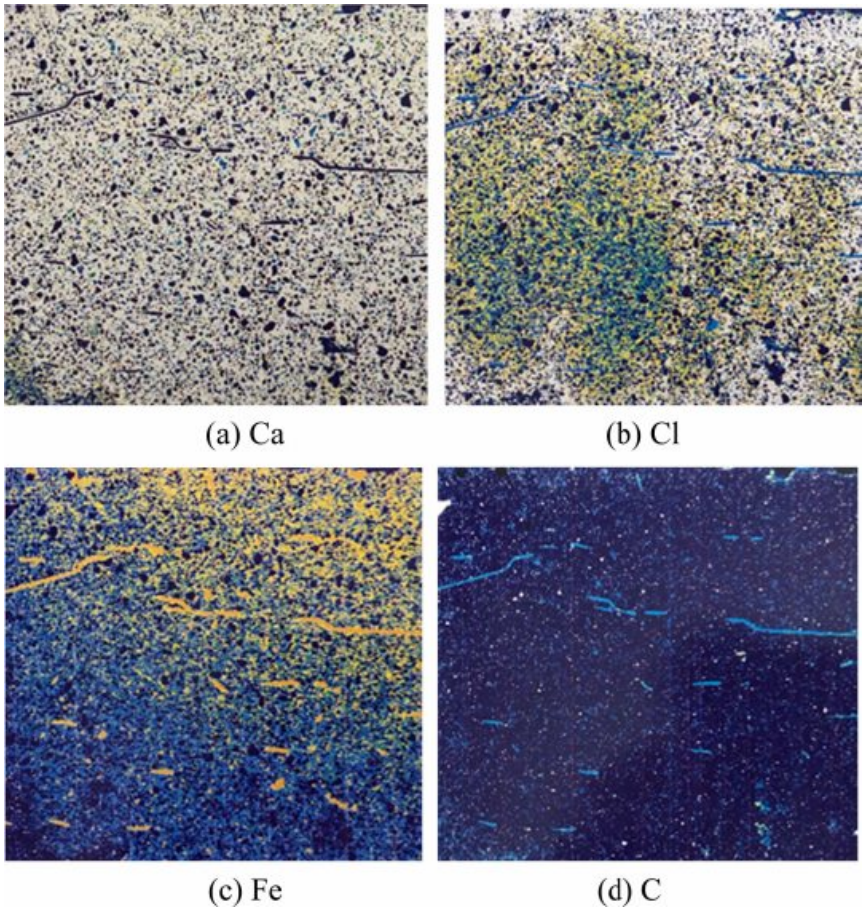


**Fig. 13.** Cl ions behavior on the M3 specimens (EPMA).

3) It was found that swelling and expansion additives significantly affected the formation of re-hydration products on self-healing capabilities as well as anti-corrosion properties. From these new concepts, some particular mix-proportions for inorganic anti-corrosion agents with self-healing capabilities were suggested.

## Acknowledgments

This paper was sponsored by Wonkwang University in 2019.

## References

1. B. Elsener, Cement and Concrete Composite. 24 (2002) 65-72.
2. J.M. Gaidis, Cement and Concrete Composite. 26 (2004) 181-189.
3. K. Petterson, Corrosion and Corrosion Protection of Steel in Concrete; Swamy, R.N., Ed.; Academic Press: Sheffield, UK, (1994) 461.
4. M. Koichi, M Morioka, T. Koji, Cement Science and Concrete Technology, 68, 218-225.
5. B.C. Moon, J.H. Yoo, H.S. Lee, M.S. Lee, AIK. 25[1] (2009) p. 113-121.
6. H.Y. Moon, Korea Concrete Institute 10[6] (1998) 325-334
7. K.B. Shim, T. kishi, C.S. Choi, T.H. Ahn, JCPR 16[1] (2015) 1-13.
8. T. kishi, T.H. Ahn, Journal of Advanced Concrete Technology 8[2] (2008) 171-186.
9. F.R. Abro, A.S. Buller, K.M. Lee, S.Y. Jang, Materials, 12 (2019) 1865.
10. B. Van Belleghem, S. Kesser, N. De Belie, Cement and Concrete Research 113 (2018) 130-139.
11. Dessi A. Koleva, Materials 11 (2018) 309.
12. P. Azarsa, R. Gupta, A. Biparva, Cement and Concrete Composites 99 (2019) 17-31.
13. C. De Nardi, S. Bullo, L. Ferrara, L. Rochin, A. Vavasori, Materials Structure 50 (2017) 191.
14. B. Park, Y.C. Choi, Construction Building Materials, 184 (2018), 1-10.
15. K.J. Shin, W. Bae, S.W. Choi, M.W. Son, K.M. Lee, Construction and Building Materials, 151 (2017), 907-915.
16. H.X.D. Lee, H.S. Wong, N.R. Buenfeld, Cement and Concrete Research 79 (2016) 194-208.
17. G. Souradeep, H.W. Kua, Journal of Materials in Civil Engineering, 28 (2016) 04016165.
18. E. Cuenca, A Tejedor, L. Ferrara, Construction and Building Materials, 179 (2018) 619-632.
19. H. Mihashi, T. Nishiwaki, Journal of Advanced Concrete Technology, 10 (2012) 170-184.
20. S.H. Bae, Y.S. Jung, J.D. Ha, KIC 23[5] (2008) 815-824.